Low-temperature polaronic relaxations with variable range hopping conductivity in $FeTiMO_6$ (M = Ta,Nb,Sb)

S. K. Deshpande,[1,*] S. N. Achary,[2] Rohini Mani,[3] J. Gopalakrishnan,[3] and A. K. Tyagi[2]

[1]*University Grants Commission-Department of Atomic Energy Consortium for Scientific Research, R5 Shed, Bhabha Atomic Research Centre, Mumbai 400085, India*

[2]*Chemistry Division, Bhabha Atomic Research Centre, Mumbai 400085, India*

[3]*Solid State and Structural Chemistry Unit, Indian Institute of Science, Bangalore 560012, India*

(Received 27 April 2011; published 18 August 2011)

Low-temperature dielectric measurements on $FeTiMO_6$ (M = Ta,Nb,Sb) rutile-type oxides at frequencies from 0.1 Hz to 10 MHz revealed anomalous dielectric relaxations with frequency dispersion. Unlike the high-temperature relaxor response of these materials, the low-temperature relaxations are polaronic in nature. The relationship between frequency and temperature of dielectric loss peak follows $T^{-1/4}$ behavior. The frequency dependence of ac conductivity shows the well-known universal dielectric response, while the dc conductivity follows Mott variable range hopping (VRH) behavior, confirming the polaronic origin of the observed dielectric relaxations. The frequency domain analysis of the dielectric spectra shows evidence for two relaxations, with the high-frequency relaxations following Mott VRH behavior more closely. Significantly, the Cr- and Ga-based analogs, $CrTiNbO_6$ and $GaTiMO_6$ (M = Ta,Nb), that were also studied, did not show these anomalies.

DOI: 10.1103/PhysRevB.84.064301 PACS number(s): 77.22.Gm, 71.38.Ht, 72.80.Ng, 77.80.Jk

I. INTRODUCTION

Rutile (TiO_2) and oxides based on the rutile structure are being extensively studied due to their interesting physical and chemical properties.[1] Rutile represents a generic inorganic structure adopted by several metal oxides of MO_2, $MM'O_4$, and $MM'M''O_6$ stoichiometries. The dielectric properties of the Ti^{4+} containing oxides are particularly interesting due to the d^0 electronic configuration of Ti^{4+}. Rutile TiO_2 is also classified as an incipient ferroelectric, with a large static dielectric permittivity and soft (A_{2u}) mode.[2] The transition metal oxides with d^0 configuration exhibit a second-order Jahn-Teller (SOJT) distortion of the MO_6 (M = metal) octahedra, arising from the mixing of the empty d^0 states of the metal with the oxygen $2p$ states.[3,4] The phase transitions arising from the SOJT are normally reflected in the various physicals properties, like conductivity and dielectric behavior.

In order to generalize the dielectric properties of rutile type oxides, we had carried out systematic studies on several $MM'O_4$ and $MM'M''O_6$ type compositions. Recently, we have reported ferroelectric and relaxorlike response, with a relatively large permittivity and transition temperature about 550 K, in the rutile-based compound $FeTiTaO_6$.[5] Later studies by Shi *et al*. have further confirmed the relaxor response of $FeTiTaO_6$.[6] Studies on other rutile-based compounds $MM'O_4$ and $MTiM''O_6$ (M = Fe,Cr,Ga, M' = Ta,Nb,Sb) revealed that the $MTiM''O_6$ oxides with M = Fe, Cr show relaxorlike behavior at elevated temperatures, with a more pronounced effect in the Fe-containing compounds.[7] In contrast, the Ga-based compounds and the two $MM'O_4$ compounds studied ($FeTaO_4$ and $CrTaO_4$) did not show any relaxations up to 600 K. From our studies and the results reported by Shi *et al*. (Ref. 6), it is believed that Fe plays a vital role in the relaxor ferroelectricity, since the contribution of the oxygen vacancies is insignificant.

At low temperatures, polaronic relaxation has been reported for several high-permittivity materials, like $CaCu_3Ti_4O_{12}$,[8] A_2FeNbO_6 (A = Ba,Sr,Ca),[9–11] and La_2CoMnO_6.[12] In addition relaxor ferroelectric behavior at high temperature was also reported in $CaCu_3Ti_4O_{12}$.[13,14] It is therefore of interest to determine if similar processes exist in the rutile-based compounds showing relaxor ferroelectric behavior, which are important due to their potential for developing lead-free relaxor ferroelectrics.[15] Also, all the earlier studies on rutile-type $MM'O_4$ or $MM'M''O_6$ mainly concentrated only on the high-temperature properties. In order to gain further insight into the processes responsible for the dielectric relaxations of these materials, more detailed studies over wider temperature and frequency ranges are essential.

In this paper, we report the results of our studies on the low-temperature dielectric behavior of the $ATiMO_6$ (A = Fe,Ga,Cr, M = Ta,Sb,Nb) compounds. We have found evidence of polaronic relaxation in the compositions containing Fe, but no such relaxation was observed in the Ga and Cr containing compositions. Our observations suggest that Fe plays a crucial role in the dielectric relaxation. The ease in change of oxidation states of Fe suggests that the polaron hopping at low temperature is due to presence of heterovalent Fe ions. The differences in the redox behavior between Ta^{5+}, Nb^{5+}, and Sb^{5+} affect the polaron dynamics, leading to differences in the observed relaxation behavior.

II. EXPERIMENT

The $ATiMO_6$ oxides (A = Fe,Ga,Cr, M = Ta,Nb,Sb) were synthesized by conventional solid-state methods with appropriate starting materials. Details of the synthesis and structural characterization by x-ray diffraction and neutron diffraction have been reported elsewhere.[7] Dielectric measurements were carried out on the samples in cylindrical pellet form using a Novocontrol Alpha impedance analyzer (Novocontrol Technologies, Germany) equipped with a Quatro liquid nitrogen gas cryosystem, over a frequency range of 0.1 Hz to 10 MHz at several temperatures between −150 °C and +20 °C. Silver paint was applied to the pellet surface for proper electrical contact. Analysis of the data was carried out with the help of the WinFIT software (Novocontrol Technologies).

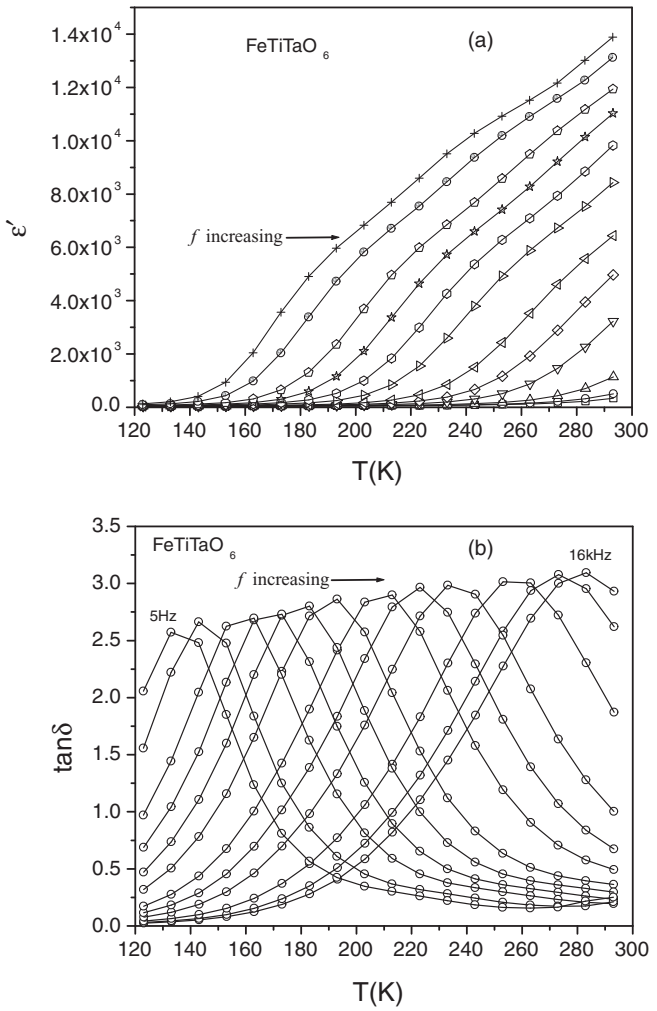

FIG. 1. Temperature dependence of the dielectric constant ε' (a) and tanδ (b) for $FeTiTaO_6$ at select frequencies. Lines are to guide the eye.

III. RESULTS AND DISCUSSION

Temperature-dependent dielectric constant ε' (real part of complex relative permittivity) and loss factor (tanδ) of all the materials investigated were extracted from the analysis of the impedance data. The variation of dielectric constant and loss factor with temperature is shown in Fig. 1 for $FeTiTaO_6$ at select frequencies. A dielectric anomaly showing strong frequency dispersion can be clearly seen. The relative permittivity drops from around 10^4 to 55 as temperature is reduced from 300 K to 120 K at 100 Hz [Fig. 1(a)]. Figure 1(b) shows that the temperature (T_m), corresponding to the peak in tanδ, shifts towards higher values as the frequency increases. A similar shift of T_m was observed in the temperature-dependent loss factors of $FeTiNbO_6$ and $FeTiSbO_6$, as shown in Fig. 2. No such anomalous behavior was observed for the Ga- and Cr-containing compounds (see Fig. 2(c)).

Further analysis of the frequency-dependence of T_m of these Fe bearing materials was carried out by fitting the data to the Arrhenius relation

$$f = f_0 \exp(-\Delta E / k_B T_m), \quad (1)$$

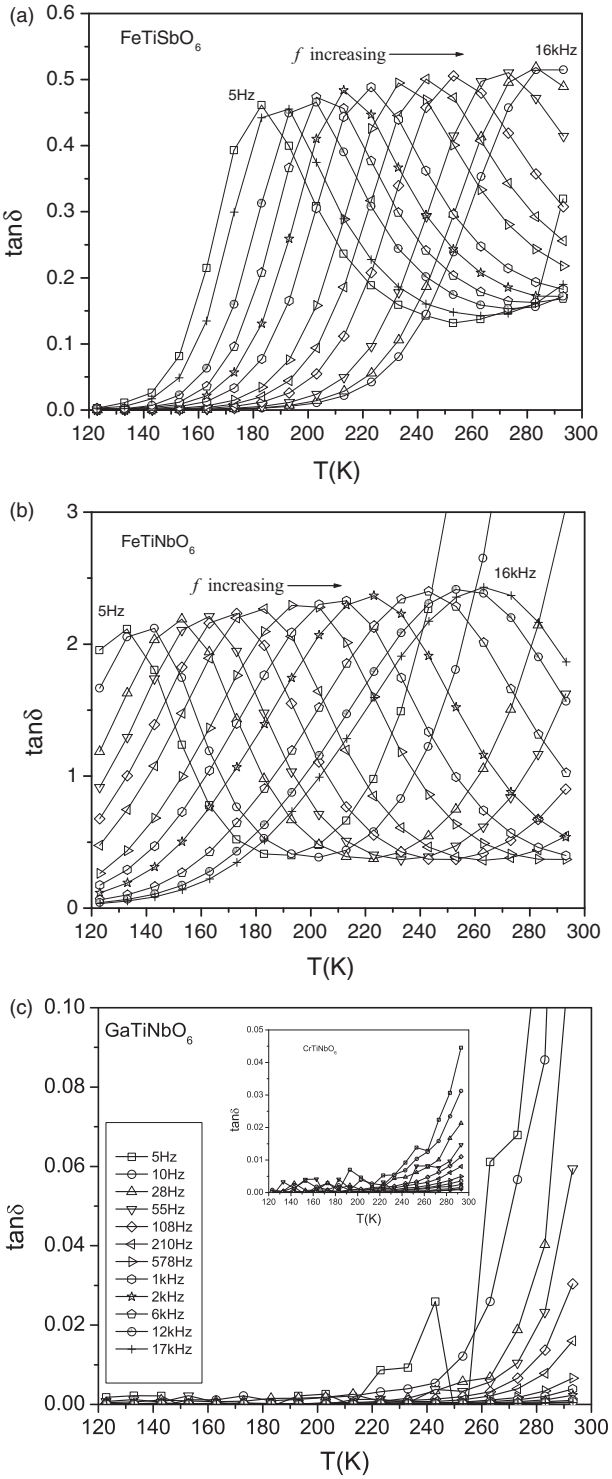

FIG. 2. Temperature dependence of tanδ for (a) $FeTiSbO_6$, (b) $FeTiNbO_6$, and (c) $GaTiNbO_6$ at select frequencies. Inset of Fig. 2(c) shows the temperature dependence of tanδ for $CrTiNbO_6$. Lines are a guide to the eye.

where f is the frequency, f_0 is a pre-exponential term, k_B the Boltzmann constant, and ΔE is the activation energy. The best-fit values of ΔE and f_0 for $FeTiTaO_6$ were 0.18 eV and 1.69×10^7 Hz, respectively. The corresponding values for $FeTiNbO_6$ are 0.19 eV and 5.13×10^7 Hz, and for $FeTiNbO_6$ they are 0.35 eV and 1.95×10^{10} Hz, respectively. These

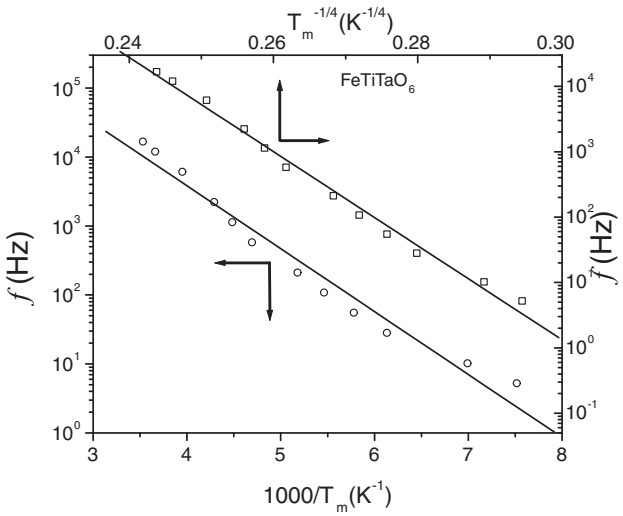

FIG. 3. Relation between frequency f and T_m, the temperature at tanδ peak in $FeTiTaO_6$. Solid lines are fits to the Mott VRH model (upper scale) and to the Arrhenius model (lower scale).

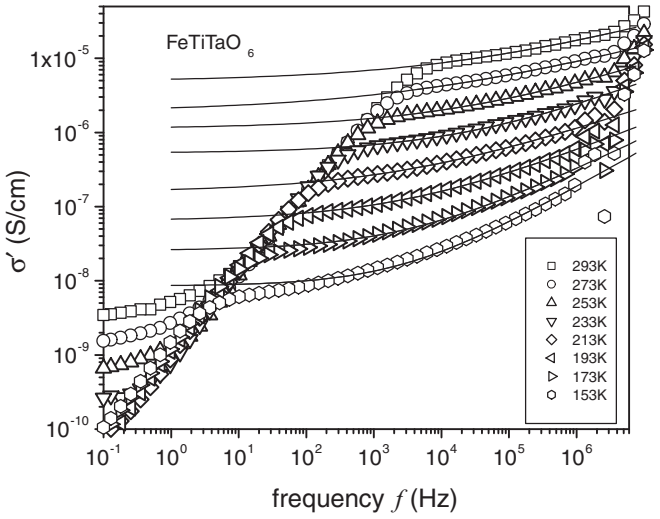

FIG. 4. Conductivity vs frequency at several temperatures for $FeTiTaO_6$. The symbols are experimental data, and solid lines are fits to the UDR model.

values are close to those obtained for dielectric relaxation in the well-known electronic ferroelectrics like $LuFe_2O_4$.[16] The perovskite-type A_2FeNbO_6 (A = Ba,Ca,Sr) oxides[9–11] show similar relaxation behavior, and the reported values of ΔE and f_0 are also similar to those observed for the $FeTiMO_6$ in our study. A closer look at the experimental data of $FeTiMO_6$ shows significant deviations from the Arrhenius straight line, as seen in Fig. 3 (lower scale, open circles). Such deviations from Arrhenius behavior have been found in several materials, showing polaronic conduction.[17,18] The origin of such deviations from Arrhenius behavior in the present studied materials may be attributed to the polaronic origin of relaxation. A much better fit to the experimental data could be obtained by using the relation

$$f = f_0 \exp[-(T_0/T_m)^{1/4}], \tag{2}$$

where f_0 and T_0 are fitting parameters. The fit to this model is shown in Fig. 3 (upper scale, open squares). This suggests a polaronic origin of the low-temperature dielectric relaxations in the $FeTiMO_6$ compounds. The values of f_0 and T_0 were found to be 5.13×10^{21} Hz and 7.55×10^8 K, for $FeTiTaO_6$, 1.82×10^{23} Hz and 9.79×10^8 K for $FeTiNbO_6$, and 1.82×10^{33} Hz and 5.73×10^9 K, for $FeTiSbO_6$, respectively.

It may be noted that for the high-temperature dielectric relaxation in these Fe-based materials, the frequency dependence of T_m was found to follow the Vogel-Fulcher behavior, which is a characteristic of relaxor ferroelectrics.[5–7] This is not the case for the low-temperature relaxations, as discussed above, implying that the observed low-temperature relaxations are obviously not relaxorlike.

It is well known that at low temperatures, conductivity arising from thermally assisted tunneling between localized states, as in polaronic conduction, follows the Mott variable range hopping (VRH) model.[19] In this model, the dc conductivity can be described by the relation

$$\sigma_{dc} = \sigma_0 \exp[-(T_1/T)^{1/4}], \tag{3}$$

where σ_0 and T_1 are constants. T_1 is given by

$$T_1 = 24/[\pi k_B N(E_F) \xi^3], \tag{4}$$

where $N(E_F)$ is the density of localized states at the Fermi level, and ξ is the decay length of the localized wave function. The activation energy W at a particular temperature T is given by

$$W = 0.25 k_B T_1^{1/4} T^{3/4}, \tag{5}$$

and the hopping range of polarons (R) is given by

$$R = \xi^{1/4}/[8\pi k_B N(E_F) T]^{1/4}. \tag{6}$$

Thus, a $T_m^{-1/4}$ dependence of the relaxation frequency [Eq. (2)] suggests the Mott VRH behavior, assuming a linear relation between relaxation frequency and the dc conductivity.[17]

In order to verify the polaronic nature of the relaxations, we have extracted the dc conductivity from the experimentally observed ac conductivity at several temperatures, as shown in Fig. 4. The low-frequency region, showing a sharp frequency-dependent increase in conductivity is the contribution from the grain boundaries. The slowly varying (nearly flat) region at the top of each curve is the bulk contribution, which is known to follow the universal dielectric response (UDR)[20]

$$\sigma = \sigma_{dc} + \sigma_0^{UDR} f^s, \tag{7}$$

where σ_{dc} is the bulk dc conductivity, σ_0^{UDR} is a constant, f is the frequency, and s is an exponent smaller than 1. Equation (7) is a common feature of all amorphous semiconductors and many materials exhibiting disorder.[21]

Fitting Eq. (7) to the high-frequency region of the data yielded σ_{dc}, σ_0^{UDR}, and s at different temperatures. The

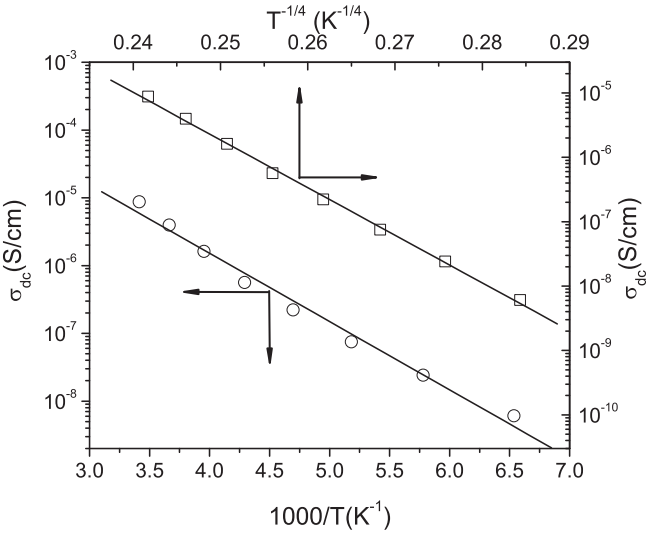

FIG. 5. Temperature dependence of dc conductivity in $FeTiTaO_6$. Solid lines are fits to the Mott VRH model (upper scale) and the Arrhenius model (lower scale).

temperature dependence of σ_{dc} thus obtained was analyzed by fitting the data to the Arrhenius relation

$$\sigma_{dc} = \sigma_1 \exp(-E_a/k_B T), \tag{8}$$

where σ_1 is a pre-exponential factor, and E_a is the activation energy for hopping conduction. Similar to the temperature dependence of T_m (Fig. 3, lower curve), there is significant deviation from the Arrhenius relation. However, very good fit was obtained when the Mott VRH relation [Eq. (3)] was used. These results are depicted in Fig. 5 for $FeTiTaO_6$. The best-fit values of σ_0 and T_1 for $FeTiTaO_6$ are 5.9×10^{12} S/cm and 8.43×10^8 K, respectively. The extracted value of T_1 is close to that reported in literature for the double-perovskites La_2CoMnO_6[12] and La_2NiMnO_6.[22]

The average cation-oxygen (M-O) distance in $FeTiTaO_6$ is 1.992 A.[5] The average cation-cation distance can be taken as twice this value, which is 3.984 A. Taking this as the decay length ξ, and using Eq. (4), the value of $N(E_F)$ was found to be 1.66×10^{18} eV/cm^3. These values of ξ and $N(E_F)$ can be inserted in Eq. (6) to obtain the hopping range R in $FeTiTaO_6$. We find that the hopping range decreases monotonically with temperature from 54.8 A at 123 K to 44.1 A at 293 K. Using Eq. (5), we obtain the activation energy W as 0.14 eV at 123 K and 0.26 eV at 293 K. These values of R and W satisfy the conditions $R \geqslant \xi$ and $W > k_B T$, respectively, which are essential for the Mott VRH model.[23]

The data for the $FeTiNbO_6$ and $FeTiSbO_6$ compositions also showed the Mott VRH behavior (see Fig. 6). Thus, the experimental data was fit to Eq. (3), and the corresponding values of σ_0 and T_1 are 1.9×10^{13} S/cm and 8.43×10^8 K for $FeTiNbO_6$ and 8.52×10^{22} S/cm and 5.66×10^9 K for $FeTiSbO_6$, respectively. Since it well known that the Mott VRH behavior is evidence for polaron hopping, we conclude that the low-temperature relaxations in $FeTiMO_6$ are indeed polaronic in nature.

The imaginary part of the complex permittivity as a function of frequency is plotted in Fig. 7(a) for $FeTiTaO_6$ at several

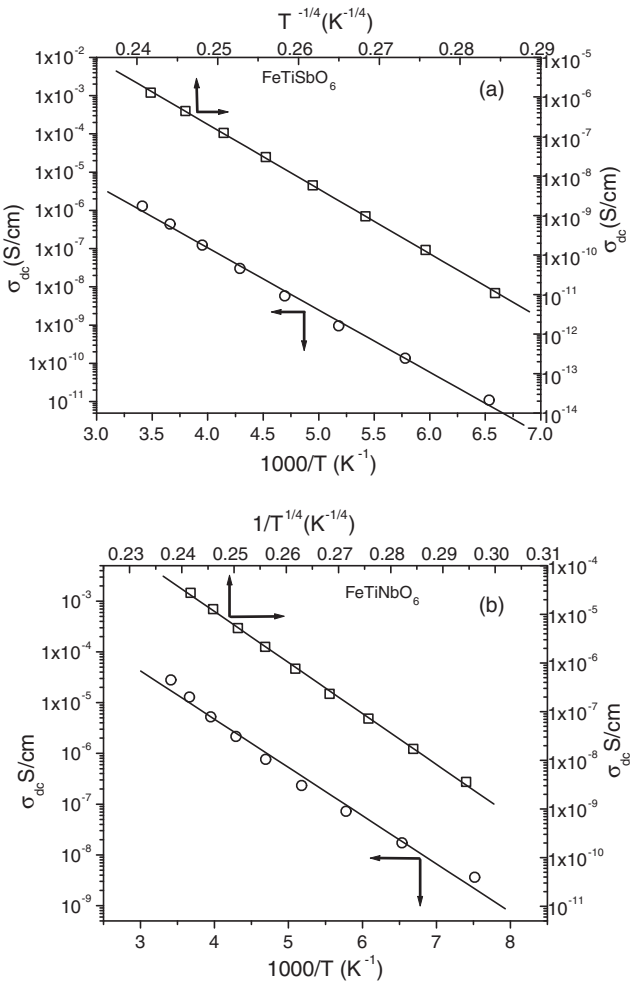

FIG. 6. Temperature dependence of dc conductivity in (a) $FeTiSbO_6$ and (b) $FeTiNbO_6$. Solid lines are fits to the Mott VRH model (upper scales) and to the Arrhenius model (lower scales).

temperatures. The frequency-dependent complex permittivity $\varepsilon^*(\omega)$ can be most generally represented by the Havriliak-Negami (H-N) model,[24] as given below

$$\varepsilon^*(\omega) = \varepsilon_\infty + (\varepsilon_s - \varepsilon_\infty)/[1 + (i\omega\tau)^\alpha]^\beta, \tag{9}$$

where $\omega = 2\pi f$ is the angular frequency, τ is the relaxation time, ε_s and ε_∞ are the low- and high-frequency values of ε', respectively, $i = \sqrt{-1}$, and α and β are exponents such that $\alpha > 0, \alpha\beta \leqslant 1$. The contribution due to electrical conductivity can be incorporated by adding the term $(-i[\sigma_{dc}\ (/\varepsilon_0\omega)]^n)$ to Eq. (9), where σ_{dc} is the dc conductivity and ε_0 is the permittivity of free space, and $n \approx 1$.

We have found that the experimental data could not be satisfactorily fit with only a single H-N relaxation and a conductivity term, but an excellent fit was obtained with two H-N functions, indicating two distinct dielectric relaxations, in addition to the conductivity contribution, as below

$$\varepsilon^*(\omega) = \varepsilon_\infty + \frac{\varepsilon_s - \varepsilon_\infty}{[1 + (i\omega\tau_1)^{\alpha_1}]^{\beta_1}} + \frac{\varepsilon_s - \varepsilon_\infty}{[1 + (i\omega\tau_2)^{\alpha_2}]^{\beta_2}} - i[\sigma_{dc}/(\varepsilon_0\omega)]^n, \tag{10}$$

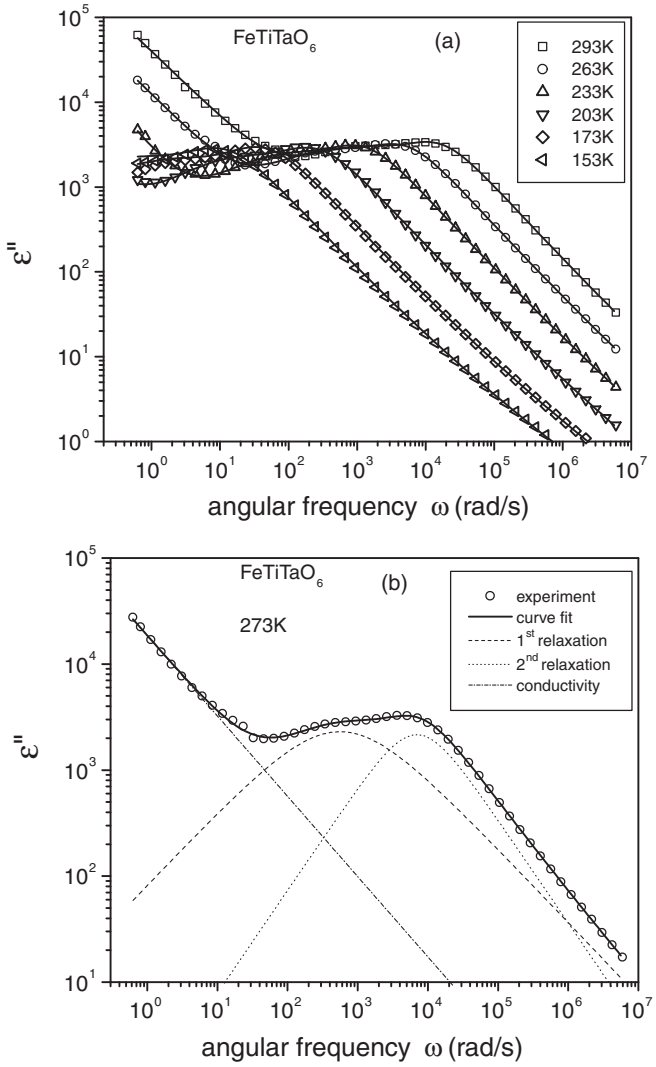

FIG. 7. (a) Dielectric loss (imaginary part of permittivity) at selected temperatures for $FeTiTaO_6$. The solid lines are fit to data according to Eq. (10) (see text). (b) Curve-fitting results showing individual contributions to the dielectric loss at 273 K for $FeTiTaO_6$.

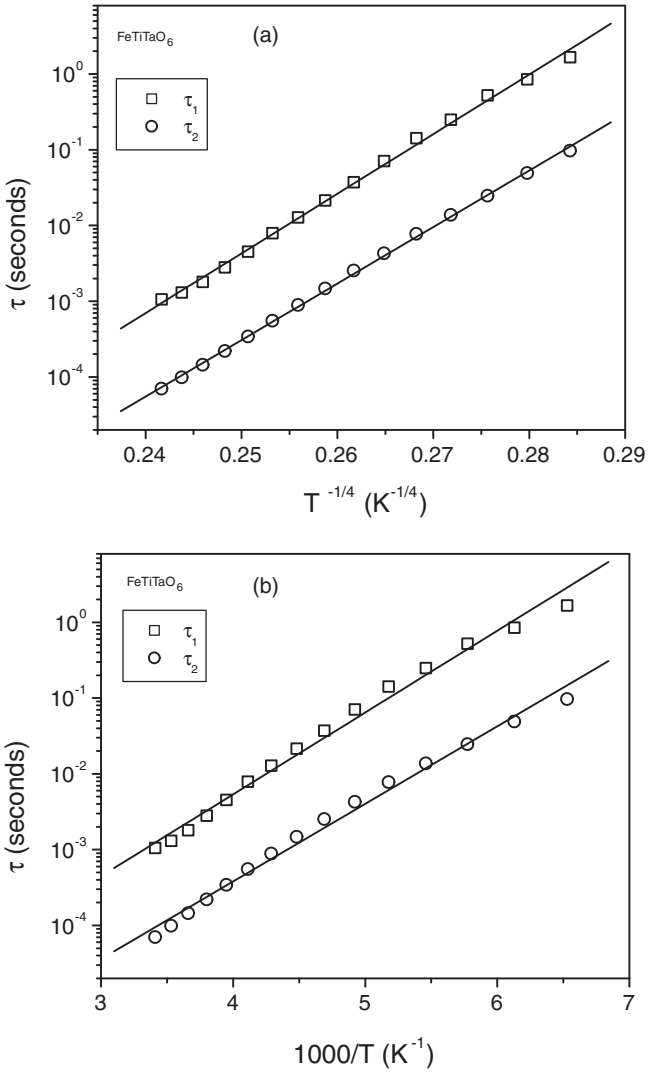

FIG. 8. The temperature dependence of the two relaxation times τ_1 and τ_2 in $FeTiTaO_6$. Solid lines are fit to (a) the Mott VRH model and (b) the Arrhenius model.

where the subscripts 1 and 2 correspond to the two relaxations, respectively.

The curve-fitting results at selected temperatures are shown in Fig. 7(a) for $FeTiTaO_6$, and a typical example of the individual relaxations is shown in Fig. 7(b) for the data at 273 K. Similarly, the dielectric loss spectra for $FeTiSbO_6$ and $FeTiNbO_6$ also showed two relaxations, although for $FeTiNbO_6$ sample, the two relaxations were not very well separated in frequency. It may be noted that two relaxations are not discernible in the tanδ curves of Figs. 1(b), 2(a), and 2(b), probably due to the width of the tanδ peaks. However, some indication of double relaxation is seen from the plot of relative permittivity [Fig. 1(a)].

The temperature dependence of the two relaxation times τ_1 and τ_2 could again be very well approximated by the Mott VRH-type relation:

$$\tau = \tau_0 \exp[(-T_1/T)^{1/4}], \qquad (11)$$

where τ_0 and T_1 are fitting parameters, and T is the temperature. Figure 8(a) shows the plots of $\log_{10}\tau_1$ and $\log_{10}\tau_2$ against $1/T^{1/4}$ for $FeTiTaO_6$. T_1 was found to be 1.1×10^9 K and 8.7×10^8 K for τ_1 and τ_2, respectively. This compares well with the value of 8.1×10^8 K for La_2CoMnO_6.[11] The corresponding values for $FeTiSbO_6$ were 9.8×10^8 K and 9.7×10^8 K, and for $FeTiNbO_6$ they were 9.9×10^9 K and 6.1×10^9 K, respectively. The data showed significant deviations from the Arrhenius behavior, as seen from the plots of $\log_{10}\tau_1$ and $\log_{10}\tau_2$ against 1000/T in Fig. 8(b). In all these compounds, the higher-frequency relaxation τ_2 shows a much better fit to Eq. (11) than the lower-frequency (longer relaxation time) relaxation τ_1. This suggests that the higher-frequency relaxations at all the temperatures studied are certainly polaronic, while the low-frequency relaxations may originate from polaron hopping or other unknown processes. The fact that the height of the tanδ peaks in Figs. 1(b), 2(a), and 2(b) does not decrease with temperatures suggests that there is no significant contribution due to Maxwell-Wagner-type

interfacial polarization. In general the Maxwell-Wagner-type polarization would lead to low-frequency relaxations, which reduce in intensity with increasing temperature. The origin of the lower-frequency (τ_1) relaxation is therefore not very clear.

It is interesting to note that the polaronic relaxations in several materials are associated with charge ordering of ions in the lattice. For example, the coexistence of Ti^{3+} and Ti^{4+} is believed to cause polaronic effects in $CaCu_3Ti_4O_{12}$.[17] In La_2MMnO_6 (M = Co,Ni), the charge ordering of M^{2+} and Mn^{4+} is believed to induce local polar behavior.[12] In fact, electronic ferroelectricity is believed to originate from ordering of Fe^{2+} and Fe^{3+} in $LuFe_2O_4$,[16] while in the double perovskites A_2FeNbO_6 (A = Ba,Sr,Ca), the low-temperature relaxations are caused by ordering of heterovalent Fe ions.[9–11] The Ga- and Cr-containing compositions in our study do not show any relaxations at low temperatures, while the Fe-based compositions show polaronic relaxations. The fact that heterovalency of Fe ions can exist in Fe-based compounds suggests that charge ordering of heterovalent Fe ions leads to the observed polaronic relaxations in $FeTiMO_6$.

The polaronic relaxation is thus observed only in the Fe-containing compositions. The polaron dynamics in the $FeTiTaO_6$, $FeTiNbO_6$, and $FeTiSbO_6$ compositions are related to the nature of charge balancing counterions, like Ta^{5+}, Nb^{5+}, and Sb^{5+} ions. The samples prepared at high temperature can easily lead to oxygen vacancies in the lattice due to a partial formation of Fe^{2+} in the lattice. The possible interactions of Fe^{2+} with other ions leads to Fe^{2+}-M^{5+} (M = Ta, Nb, Sb), Fe^{2+}-Ti^{4+}, and Fe^{2+}-$[V]_O$ (oxygen vacancies) pairs, and the stabilities of these pairs are reflected in the difference in the relaxation dynamics of the materials. It can be easily understood that the contribution from the Ti^{4+} will remain comparable in all the compositions. Thus, the redox potential of the M^{5+} ion and stability of the oxygen vacancies are the reasons for the observed difference in relaxation behavior. By a simple analogy of the redox behavior of Ta^{5+}, Nb^{5+}, and Sb^{5+}, it can be easily concluded that the Ta^{5+} and Sb^{5+} will exhibit two extreme behaviors than the Nb^{5+}. Since Ta^{5+}-Ta^{4+} redox couple has higher energy compared to Nb^{5+}-Nb^{4+} redox couple, the easy formation of Nb^{4+} is expected compared to Ta^{4+}. Thus, the two distinct relaxations observed in $FeTiTaO_6$ [Fig. 7(b)] may be attributed to the appreciable difference in the stability of the polarons in two different defect pairs in $FeTiTaO_6$ compared to the $FeTiNbO_6$. The situation in $FeTiSbO_6$ is further different due to the possibilities of redox processes like Sb^{5+}-Sb^{4+}-Sb^{3+} (involving 1 and 2 electrons). These dissimilarities in the three compounds are reflected in the different best-fit values of σ_0 and T_1 of the VRH model. Also, they result in different τ_1 and τ_2 values in the studied compositions.

We would like to mention here that the possibility of charge ordering in $FeTiTaO_6$ was indicated by the neutron diffraction measurements reported earlier,[5] where a weak, reflection near $2\theta = 15^\circ$ was observed. These were absent in the corresponding data for $CrTiTaO_6$, which is not expected to show charge ordering. However, more detailed refinement of the structural data is needed to confirm this.

IV. CONCLUSION

We have found low-temperature dielectric anomalies originating from polaron hopping in $FeTiMO_6$ (M = Ta,Nb,Sb) rutile-based compounds. The relationship between temperature at the dielectric loss peak and the relaxation frequency, as well as the temperature dependence of dc conductivity, show deviations from Arrhenius behavior. The dc conductivity follows the Mott VRH behavior. The Ga- and Cr-based analogs did not show this type of dielectric behavior, which highlights the importance of Fe ions in determining the interesting dielectric properties of these materials. Our observations suggest the charge-ordering of heterovalent Fe ions leads to the polaronic effects, with the charge fluctuation balanced by oxygen vacancies. Frequency domain analysis of the data shows two dielectric relaxations following the general H-N model. Of the two relaxations observed in frequency domain, the higher-frequency relaxations show typical VRH behavior, while the low-frequency relaxations show some deviation.

ACKNOWLEDGMENTS

JG thanks the Department of Science and Technology and the Indian National Science Academy, New Delhi for support. AKT thanks Department of Atomic Energy's Science Research Council (DAE-SRC) for supporting this work via Grant No. 2010/21/9-BRNS.

*skdesh@barc.gov.in

[1] W. H. Baur, Crystallogr. Rev. **13**, 65 (2007).
[2] C. Lee, P. Ghosez, and X. Gonze, Phys. Rev. B **50**, 13379 (1994).
[3] P. S. Halasyamani and K. R. Poeppelmeier, Chem. Mater. **10**, 2753 (1998).
[4] N. S. P. Bhuvanesh and J. Gopalakrishnan, J. Mater. Chem. **7**, 2297 (1997).
[5] R. Mani, S. N. Achary, K. R. Chakraborty, S. K. Deshpande, J. E. Joy, A. Nag, J. Gopalakrishnan, and A. K. Tyagi, Adv. Mater. Weinheim **20**, 1348 (2008).
[6] Y. Shi, Y.-D. Hou, C. Wang, H.-Y. Ge, and M.-K. Zhu, J. Am. Ceram. Soc. **93**, 2491 (2010).
[7] R. Mani, S. N. Achary, K. R. Chakraborty, S. K. Deshpande, J. E. Joy, A. Nag, J. Gopalakrishnan, and A. K. Tyagi, J. Solid State Chem. **183**, 1380 (2010).
[8] C. C. Wang and L. W. Zhang, Appl. Phys. Lett. **90**, 142905 (2007).
[9] S. Ke, H. Fan, and H. Huang, J. Electroceram. **22**, 252 (2009).
[10] Y. Y. Liu, X. M. Chen, X. Q. Liu, and L. Li, Appl. Phys. Lett. **90**, 192905 (2007).
[11] Y. Y. Liu, X. M. Chen, X. Q. Liu, and L. Li, Appl. Phys. Lett. **90**, 262904 (2007).
[12] Y. Q. Lin and X. M. Chen, J. Am. Ceram. Soc. **94**, 782 (2011).

[13]S. M. Ke, H. T. Huang, and H. Q. Fan, Appl. Phys. Lett. **89**, 182904 (2006).
[14]H. Yu, H. Liu, H. Hao, L. Guo, C. Jin, Z. Yu, and M. Cao, Appl. Phys. Lett. **91**, 222911 (2007).
[15]L. E. Cross, Nature **432**, 24 (2004).
[16]N. Ikeda, H. Ohsumi, K. Ohwada, K. Ishii, T. Inami, K. Kakurai, Y. Murakami, K. Yoshi, S. Mori, Y. Horibe, and H. Kito, Nature **436**, 1136 (2005).
[17]L. Zhang and Z.-J. Tang, Phys. Rev. B **70**, 174306 (2004).
[18]O. Bidault, M. Maglione, M. Actis, M. Kchikech, and B. Salce, Phys. Rev. B **52**, 4191 (1995).
[19]N. F. Mott and E. A. Davis, *Electronic Processes in Non-Crystalline Materials* (Clarendon, Oxford, 1979).
[20]A. K. Jonscher, *Dielectric Relaxation in Solids* (Chelsea, London, 1983).
[21]S. R. Elliott, Adv. Phys. **36**, 135 (1987).
[22]Y. Q. Lin, X. M. Chen, and X. Q. Liu, Solid State Commun. **149**, 784 (2009).
[23]A. Yildiz, S. B. Lisesivdin, M. Kasap, and D. Mardare, Physica B **404**, 1423 (2009).
[24]A. Schönhals and F. Kremer, in *Broadband Dielectric Spectroscopy*, edited by F. Kremer and A. Schönhals (Springer Verlag, Berlin, 2003), p. 63.